CONF-790150--6

RLO-1388-777

Testing Quantum Chromodynamics in Electron-Positron Annihilation at High Energies

Lowell S. Brown

University of Washington, Seattle, Washington 98195

PREPARED FOR THE U. S. DEPARTMENT OF ENERGY

RLO-1388-777

Testing Quantum Chromodynamics in Electron-Positron Annihilation at High Energies*

(Lecture presented at the 1979 Coral Gables Orbis Scientiae)

Lowell S. Brown

Department of Physics
University of Washington
Seattle, Washington 98195

Various measures of the distribution of hadronic energy produced in high-energy electron-positron annihilation provide precise tests of the promising fundamental theory of hadronic physics, quantum chromodynamics. Recent work at the University of Washington on such energy cross sections is reviewed.

*Work supported in part by the U.S. Department of Energy.

DISCLAIMER

Quantum chromodynamics is amenable to precise experimental verification. This happy state of affairs occurs because the theory is asymptotically free. At high energy W it is described by an effective running coupling

$$\bar{g}(W)^2 \sim \frac{1}{\ln W} \qquad (1)$$

which vanishes as the energy increases. Therefore, certain suitably selected, high-energy processes can be computed using perturbative methods. The now classic processes for such tests involve deep inelastic lepto-production off nuclear targets. Unfortunately, only the energy variation of these cross sections is predicted with no prediction being made for their absolute magnitudes and shapes. Recently, however, a new method has been developed which provides a more complete description. This is the method of asymptotically free perturbation theory. A large impetus for its development came from the work of Sterman and Weinberg[1].

The basic ideas of the new method are as follows. Using the total energy W to set the length scale, a partial cross section can be written in terms of a dimensionless function of dimensionless variables,

$$\Delta\sigma = \frac{1}{W^2} F\left(\frac{W}{\mu}, g_\mu^2, \frac{m_\mu^2}{\mu^2}, x\right). \qquad (2)$$

Here μ is the mass scale of the renormalization point, g_μ is the value of the renormalized coupling at this renormalization point, and m_μ is the (quark) mass treated as another coupling constant normalized at μ. The symbol x stands for the remaining dimensionless variables such as scattering angles. The physically measurable partial cross section $\Delta\sigma$ must be independent of the value of the arbitrary renormalization point μ. Hence we may take $\mu = W$, turning g_μ^2 into the running coupling $\bar{g}(W)^2$ of the renormalization group. With this choice $\frac{m_\mu^2}{\mu^2}$ is replaced by $\frac{\bar{m}(W)^2}{W^2}$ which, up to logarithmic corrections, vanishes as $1/W^2$ as the energy W becomes large. Therefore, neglecting terms which are essentially of order $1/W^2$, we secure the high energy limit

$$\Delta\sigma = \frac{1}{W^2} F(1, \bar{g}(W)^2, 0, x). \qquad (3)$$

The existence of the limit (3) requires that the partial cross section be finite in a theory with massless particles. This will generally not be the case. We must restrict our considerations to "proper processes" which are free of infrared mass divergences. This requires that the partial cross section for a "proper process" must be insensitive to soft particle production and to the collinear branching of the massless particles. The partial cross sections will be devoid of mass singularities if they refer only to inclusive energies carried off by the particles. Energy weighting removes divergences which would otherwise arise from soft

particle production and the inclusive energy summation removes potential divergences from the collinear branching of the massless particles.

Since the running coupling $\bar{g}(W)^2$ vanishes as $W \to \infty$, the partial cross section (3) can be computed by perturbation theory. Quarks and gluons are, of course, not bound into the observed hadrons in perturbation theory. Hence we can calculate perturbatively only if $\Delta\sigma$ refers to a partial cross section for quark and gluon production and not to the production of a specific hadron. However, there is good empirical evidence to support the assumption that the produced quarks and gluons fragment into hadrons with limited transverse momenta ($p_\perp < 0.3$ GeV). The observed hadrons will therefore follow closely to the directions of their parent quark or gluon. Moreover, the energy flow in the observed hadrons will even more closely approximate the energy flow of their parent since a hadron produced at a wide angle relative to its parent direction is soft and weighted little by the energy.

Since the "proper processes" cannot refer to specific, individual hadrons they cannot, in particular, contain hadrons in the initial state; we are restricted to discuss

$$e^+e^- \to \text{hadronic matter.}$$

This reaction is described by a hierarchy[2,3,4] of energy-weighted cross sections. The first member of this hierarchy

is simply the ordinary total cross section σ. The next member is the single-energy cross section[2] $d\Sigma/d\Omega$. It describes the "antenna pattern" of the radiated hadronic energy. The single-energy cross section could be determined, for example, by measurements with a small hadronic calorimeter placed at various angular positions. If the calorimeter collects an energy ΔE in a solid angle $d\Omega$ during a time T, then $d\Sigma/d\Omega = \Delta E/(W\mathcal{L}Td\Omega)$, where $\mathcal{L}$ is the luminosity of the e^+e^- colliding beams and W is the total energy of a e^+e^- pair. The single-energy cross section obeys a sum rule reflecting energy conservation,

$$\int d\Omega \frac{d\Sigma}{d\Omega} = \sigma \ . \tag{4}$$

The third member of the hierarchy is the double-energy or energy-correlation cross section[3,4] $d^2\Sigma/d\Omega d\Omega'$. It can be measured with two calorimeters, one of solid angle $d\Omega$ in the direction $\hat{r}$, the other of solid angle $d\Omega'$ in the direction $\hat{r}'$. The two calorimeters measure the energies dE and dE' which are carried by the hadrons into these solid angles during a single event. The product of the two energies, (dEdE'), is then summed for many similar events with the sum divided by the integrated luminosity $\mathcal{L}T$, times the squared energy of each collision W^2 and the solid angle product $d\Omega d\Omega'$. This procedure defines $d^2\Sigma/d\Omega d\Omega' = \Sigma_{\text{events}}(dEdE')/\mathcal{L}TW^2 d\Omega d\Omega'$. Again we have a sum rule reflecting energy conservation,

$$\int d\sigma' \frac{d^2\sigma}{d\Omega d\Omega'} = \frac{d\sigma}{d\Omega} \quad . \tag{5}$$

Let us first consider the character of the single-energy cross section $d\sigma/d\Omega$, the hadronic "antenna pattern". The geometry for the measurement of this cross section is illustrated in Fig. 1. The cross section has been calculated[2] to order $\bar{g}(W)^2$. This involves computing the amplitudes corresponding to the Feynman graphs shown in Fig. 2. Although individual amplitudes have mass singularities, the sum of terms which constitute the cross section is finite. The discussion is simplified by considering the case where the e^+e^- beams are perfectly polarized along the magnetic field direction. In this case we have

$$\frac{d\sigma}{d\Omega} = \frac{\alpha^2}{2W^2} \sum_f 3Q_f^2 \left\{ [1 + \frac{\bar{g}(W)^2}{4\pi^2}] \sin^2\psi + \frac{\bar{g}(W)^2}{4\pi^2} [3\cos^2\psi - 1] \right\} , \tag{6}$$

where $\alpha \approx 1/137$ is the fine structure constant, Q_f is the fractional charge of a quark of flavor f (with the factor 3 accounting for the three quark colors), and ψ is the angle between the detection and magnetic field directions as shown in Fig. 1. At high energy the running coupling is given by

$$\frac{\bar{g}(W)^2}{4\pi^2} = \frac{2}{[11 - \frac{2}{3}N_f] \ln(W/\Lambda)} , \tag{7}$$

where N_f is the number of quark flavors and $\Lambda \approx 0.5$ GeV is

the scale mass determined from deep inelastic lepto-production data. The angular distribution given by Eqs. (6) and (7) is plotted in Fig. 3 for $N_f = 4$. At infinite energy there is a pure $\sin^2\psi$ distribution. As the energy is lowered, the two valleys in this distribution are filled.

The fragmentation of the quarks and gluons into the observed hadrons gives a small effect which can be treated as a correction to the basic quark-anti-quark production [the cross section of Eq. (6) with $\bar{g}(W)^2 = 0$]. We assume that the parent quark or anti-quark yields a number dn of observed hadrons in the momentum interval (d^3p) given by the scaling distribution

$$dn = \frac{(d^3p)}{E^0} f(\frac{2p_\parallel}{W}, p_\perp) , \tag{8}$$

where $p_\parallel$ and $p_\perp$ are the momentum components that are respectively parallel and perpendicular to momentum of the parent. The result of this fragmentation correction is simply to replace the coefficient of $[3\cos^2\psi - 1]$ in Eq. (6) by $\frac{\bar{g}(W)^2}{4\pi^2} + \frac{-C\langle p_\perp \rangle}{4W}$, where $C \approx 2.5$ is the coefficient of the logarithmic rise of the total hadronic multiplicity in e^+e^- collisions and $\langle p_\perp \rangle \approx 0.5$ GeV is the average transverse momentum of a produced hadron. [It should be noted that, in general, the leading fragmentation corrections to members of the energy cross section hierarchy can be treated in such a simple, analytic

manner. We see that although the fragmentation process also smears the energy pattern, filling in its minima, the fragmentation correction vanishes as 1/W as the energy increases. It vanishes much more rapidly than does the perturbative QCD effect which behaves as $1/\ln W$. Figure 4 displays the size of the fragmentation corrections at W = 10 GeV and W = 30 GeV.

At W = 30 GeV the fragmentation corrections are quite small in comparison to the QCD effect. However, as is evident from Fig. 3, the QCD effect is itself small at these energies. We need a test of QCD which is not such a small effect on a large background. This leads us to consider the energy correlation cross section[3,4] $d^2\Sigma/d\chi d\Omega'$. The geometry of the experimental arrangement is shown in Fig. 5. Since the final hadronic system is produced by an intermediate, virtual photon of spin one, the angular dependence with respect to the beam and magnetic field axes is of a characteristic form. For the case of perfect e^+e^- polarization we have

$$\frac{d^2\Sigma}{d\chi d\Omega'} = \frac{\alpha^2}{2W^2}\sum_f 3Q_f^2\left\{A(\chi)(\sin^2\theta + \sin^2\theta') + B(\chi)(\cos\chi - \cos\theta\cos\theta') + C(\chi)\right\}, \tag{9}$$

where, as shown in Fig. 5, χ is the angle between the two detectors and θ,θ' are their polar angles with respect to the magnetic field direction.

The calculation of this cross section to order $\bar{g}(W)^2$ again involves the graphs of Fig. 2, and the analytic results are presented in references 3,4. Here we shall simply note that the coefficient $C(\chi)$ vanishes and display the coefficients $A(\chi)$ and $B(\chi)$ in Figs. 6 and 8. Away from $\chi = 0, \pi$; these coefficients are of order $\bar{g}(W)^2$, and the QCD effect is not a small effect on a large background. Figures 6a, b show both the quark fragmentation and the QCD contributions to $A(\chi)$ at W = 10 GeV and W = 30 GeV. We see that at W = 30 GeV the quark fragmentation correction is small over a large angular range. The leading, order 1/W fragmentation correction to $A(\chi)$ is symmetrical about $\chi = 90^\circ$. Hence the fragmentation correction to the difference

$$D(\chi) = A(\pi-\chi) - A(\chi) \tag{10}$$

is small; of order $1/W^2$. This difference, which varies over several decades, is plotted in Fig. 7. The coefficient $B(\chi)$ has no leading order (1/W) fragmentation correction. This coefficient is shown in Fig. 8.

We have found that by using the method of asymptotically free perturbation theory we have been able to make predictions for the theory of quantum chromodynamics with essentially no free parameters, predictions which should be accessible to experimental test. Since absolute magnitudes, shapes, and energy variations of several angular distributions are predicted by the theory, their experimental

confirmation would be significant. It is, of course, extremely difficult to arrive at a completely objective and precise figure of merit for a test of a theory. An indication of the sensitivity of the energy-correlation cross section can be obtained by calculating it with massless gluons that have spin 0 rather than spin 1. This has been done recently (in fact after this lecture was initially presented) by Basham and Love[5]. Using a coupling $g\bar{q}\lambda_a\phi_a q$ rather than $\bar{g}(W)\bar{q}\gamma^\mu\lambda_a A_{\mu a} q$, they find that with $g = \bar{g}(W)$ the coefficients with scalar gluons, $A^{(\text{scalar})}(\chi)$, $B^{(\text{scalar})}(\chi)$, are roughly an order of magnitude smaller than the QCD coefficients $A^{(\text{QCD})}(\chi)$ and $B^{(\text{QCD})}(\chi)$ plotted in Figs. 6 and 8. The shape of $A^{(\text{scalar})}(\chi)$ is roughly similar to that of $A^{(\text{QCD})}(\chi)$ but, as displayed in Fig. (9), the shape of $B^{(\text{scalar})}(\chi)$ is very different from that of $B^{(\text{QCD})}(\chi)$.

Let us conclude with a remark of purely theoretical interest. In perturbation theory, the energy correlation cross section becomes singular for anti-collinear detectors ($\chi \to \pi$). In this region, the leading behavior of the cross section is given by

$$\frac{d^2\Sigma}{d\Omega d\Omega'} = \frac{d\Sigma}{d\Omega}\left\{\tfrac{1}{2}\delta(\Omega+\Omega')\left[1-g^2 c\ell n^2\infty + \tfrac{1}{2}g^4 c^2 \ell n^4\infty - \ldots\right]\right.$$
$$+ \frac{g^2}{4\pi^2}\,\frac{1}{3\pi}\,\frac{1}{1+\cos\chi}\,\ell n\left(\frac{1}{1+\cos\chi}\right) \qquad (11)$$
$$\left. - \left(\frac{g^2}{4\pi^2}\right)^2 \frac{2}{9\pi}\,\frac{1}{1+\cos\chi}\left[\ell n\left(\frac{1}{1+\cos\chi}\right)\right]^3 + \ldots\right\},$$

where $\frac{d\Sigma}{d\Omega}$ is the single energy cross section given in Eq. (6)

[with $g^2 = 0$], and ... stands for higher order terms in g^2. The $\delta(\Omega+\Omega')$ term corresponds to the zeroth order production of a quark and an anti-quark which emerge back-to-back. This term is modified by (infrared mass) divergent vertex corrections. With the introduction of proper regulators, these divergences cancel against divergences produced in the remaining terms when the cross section is integrated over a small patch of solid angle covering $\chi = \pi$. Cornwall and Tiktopoulos[6] have proven (to sixth order) that the vertex modification exponentiates as indicated in Eq. (11). The order g^2 angular term previously calculated[3,4] has been recently augmented by a calculation[7] of the leading terms in order g^4 as shown in Eq. (11). Let us suppose that the vertex modifications do indeed exponentiate, multiplying $\delta(\Omega+\Omega')$ by $e^{-\infty}$ and damping it out entirely. And let us further suppose that the remaining terms also exponentiate, giving near the anti-collinear orientation

$$\frac{d^2\Sigma}{d\Omega d\Omega'} = \frac{d\Sigma}{d\Omega}\,\frac{g^2}{4\pi^2}\,\frac{1}{3\pi}\,\frac{1}{1+\cos\chi}\,\ell n\left(\frac{1}{1+\cos\chi}\right)$$
$$\exp\left\{-\frac{g^2}{4\pi^2}\,\frac{2}{3}\,\ell n^2\left(\frac{1}{1+\cos\chi}\right)\right\} \qquad (12)$$
$$= \frac{d\Sigma}{d\Omega}\,\frac{1}{4\pi}\,\frac{d}{dc\cos\chi}\exp\left\{-\frac{g^2}{4\pi^2}\,\frac{2}{3}\,\ell n^2\left(\frac{1}{1+\cos\chi}\right)\right\}.$$

Note that Eq. (12) gives a sharp peak near $\chi = \pi$. With g^2 replaced by the running coupling $\bar{g}(W)^2$, this peak decreases in width, increases in height, and moves toward $\chi = \pi$ as the energy increases.

It is interesting that this conjectured form does, in fact, satisfy a sum rule which must be obeyed by the true g^4 [illegible]. The sum rule arises as follows: If we integrate $d^2\Sigma/d\Omega d\Omega'$ over a small patch of solid angle covering $\chi = \pi$ we get a well-defined ordinary function which can be developed in a perturbation series in g^2. Accordingly, in view of the sum rule (5), we get

$$\int_{\text{patch}} d\Omega' \frac{d^2\Sigma}{d\Omega d\Omega'} = \frac{1}{2}\frac{d\Sigma}{d\Omega}[1+C(g^2)]. \qquad (13)$$

[The factor of $\frac{1}{2}$ appears since there is an equal $O(g^0)$ contribution at $\chi = 0$ because the detectors are "transparent" and can detect the same parcel of energy.] Using Eq. (12) we see that Eq. (13) is indeed satisfied. We find that the numerical coefficients of the order g^4 and order g^2 terms in Eq. (11) are related so as to produce precisely the order g^0 result required by Eq. (13).

References

1. G. Sterman and S. Weinberg, Phys. Rev. Lett. 39, 1436 (1977).

2. C. L. Basham, L. S. Brown, S. D. Ellis, and S. T. Love, Phys. Rev. D 17, 2298 (1978).

3. C. L. Basham, L. S. Brown, S. D. Ellis, and S. T. Love, Phys. Rev. Lett. 41, 1585 (1978).

4. C. L. Basham, L. S. Brown, S. D. Ellis, and S. T. Love, Phys. Rev. D (to be published). This paper contains references to related literature.

5. C. L. Basham and S. T. Love, "Energy Correlations in Electron-Positron Annihilation: Sensitivity of Quantum Chromodynamics Tests to Gluon Spin". University of Washington report (unpublished).

6. J. M. Cornwall and G. Tiktopoulos, Phys. Rev. D 13, 3370 (1976).

7. C. L. Basham, L. S. Brown, S. D. Ellis, and S. T. Love, "Energy Correlations in Perturbative Quantum Chromodynamics: A Conjecture for All Orders", manuscript in preparation.

Figure Captions

Fig. 1. Geometry for the energy pattern experiment.

Fig. 2. Zeroth, first, and second order Feynman graphs for electron-positron annihilation.
(a) Lowest-order graph for $e^+e^- \to \gamma \to q\bar{q}$.
(b) Vertex modification.
(c) Self energy insertions.
(d) Lowest-order gluon emission graphs.

Fig. 3. QCD predictions for the normalized antenna patterns $\frac{1}{\sigma}\frac{d\sigma}{d\Omega}$ corresponding to perfectly polarized electron and positron beams with various total energies W. The long dashed curve corresponds to W=5 GeV, the short dashes to W=30 GeV, and the solid curve is for infinite W. All unit vectors and angles refer to the geometry displayed in Fig. 1.

Fig. 4. QCD and the sum of QCD and quark fragmentation (qf) contributions to the normalized energy pattern $\frac{1}{\sigma}\frac{d\sigma}{d\Omega}$ with perfectly polarized electron-positron beams of total energy (a) 10 GeV, (b) 30 GeV.

Fig. 5. Geometry for the energy-energy cross section experiment. The two detectors are stationed in directions $\hat{r}$ and $\hat{r}'$ with relative angle χ. These detector directions are respectively at angles ψ and ψ' relative to the

magnetic field direction (the polarization direction) denoted by $\hat{b}$.

Fig. 6. The QCD and quark fragmentation (qf) contributions to the A coefficient in Eq. (9) are plotted as a function of χ for total energy W of (a) 10 GeV and (b) 30 GeV. Notice that the (qf) contributions is symmetric about $\chi = 90°$ while the QCD behavior is quite asymmetric.

Fig. 7 The difference $B^{(QCD)}$ defined by Eq. (10) as a function of χ for W=10 GeV. The plot for W=30 GeV is obtained by scaling the curve displayed by the factor $\bar{g}(30)^2/\bar{g}(10)^2 = 0.73$.

Fig. 8. The coefficient $B^{(QCD)}$ of Eq. (9) as a function of χ for W=10 GeV. The plot for W=30 GeV is obtained by scaling the curve displayed by the factor $\bar{g}(30)^2/\bar{g}(10)^2 = 0.73$.

Fig. 9. The QCD and scalar theory results for the B coefficient plotted as a function of χ for W = 10 GeV.

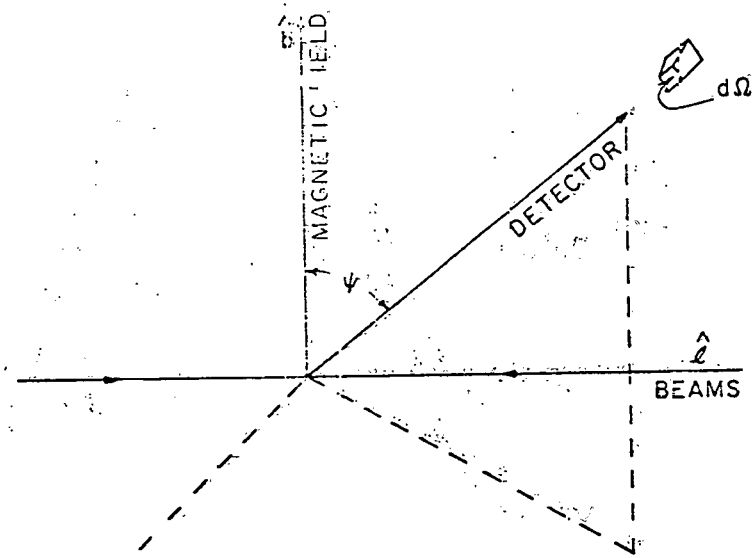

Fig. 1

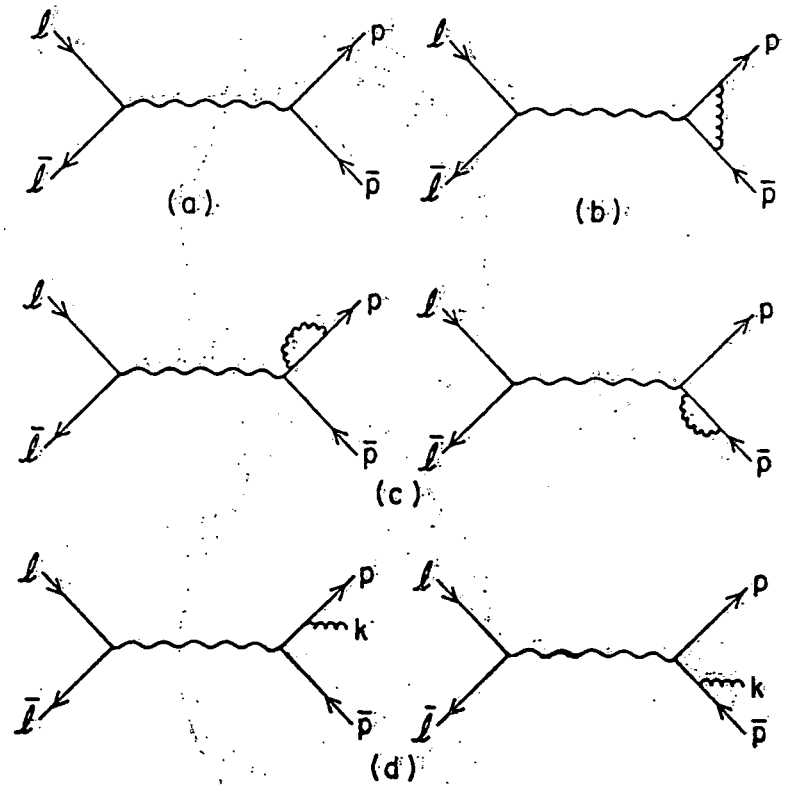

Fig. 2

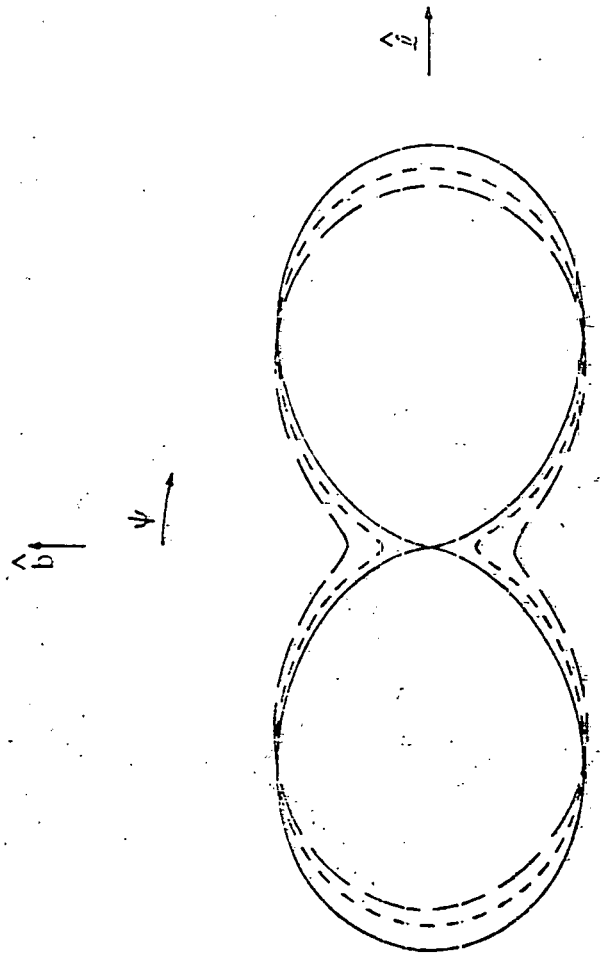
$\hat{n}$
$\hat{b}$
ψ

Fig. 3

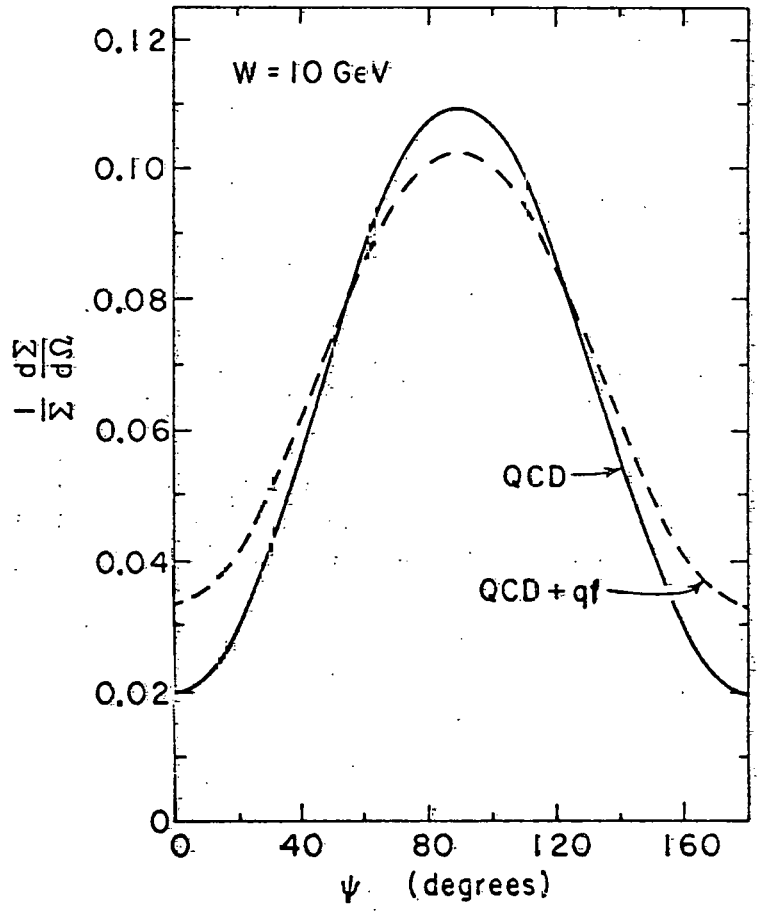
W = 10 GeV
QCD
QCD + qf
$\frac{1}{\Sigma}\frac{d\Sigma}{d\psi}$
0
0.02
0.04
0.06
0.08
0.10
0.12
0
40
80
120
160
ψ (degrees)

Fig. 4(a)

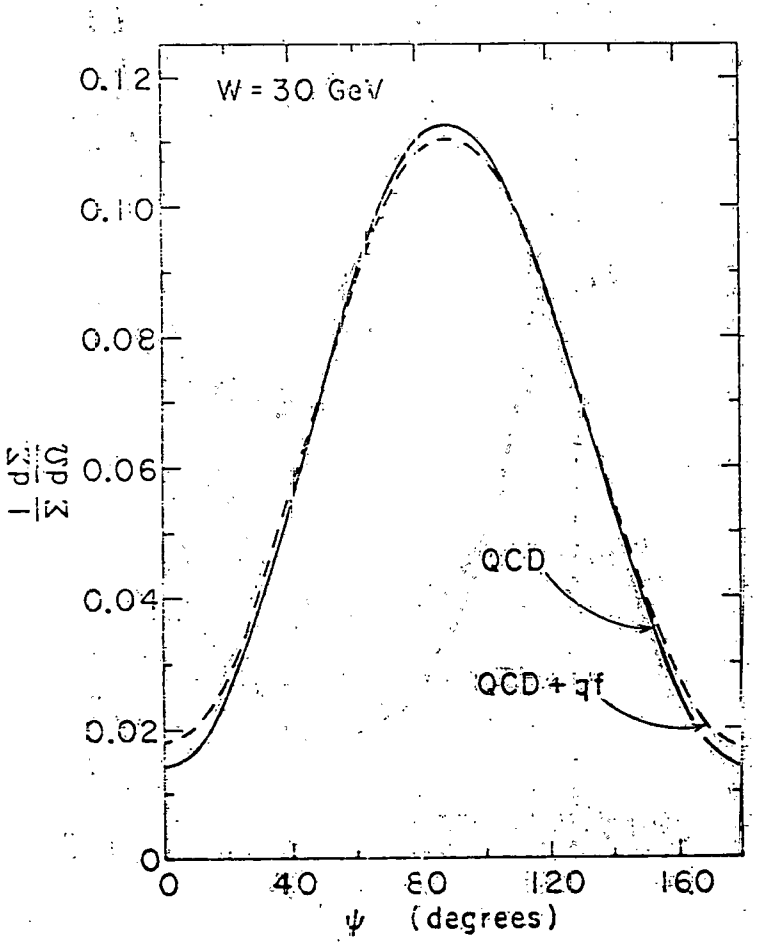
W = 30 GeV
QCD
QCD + qf
0.12
0.10
0.08
0.06
0.04
0.02
0
0
40
80
120
160
ψ (degrees)
$\frac{1}{\Sigma}\frac{d\Sigma}{d\Omega}$

Fig. 4 (b)

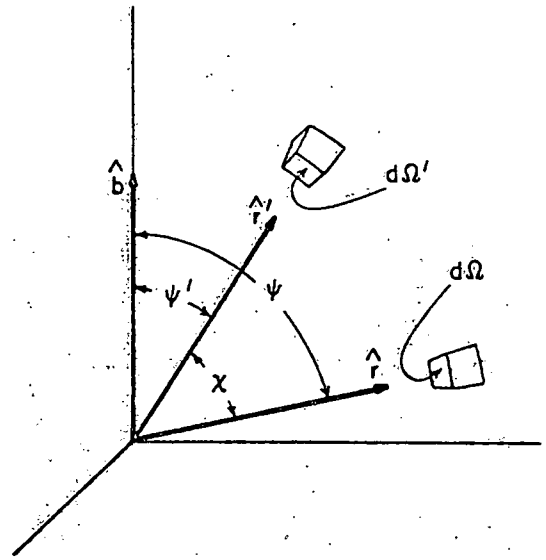
$\hat{b}$
$\hat{r}'$
$\hat{r}$
dΩ′
dΩ
ψ′
ψ
χ

Fig. 5

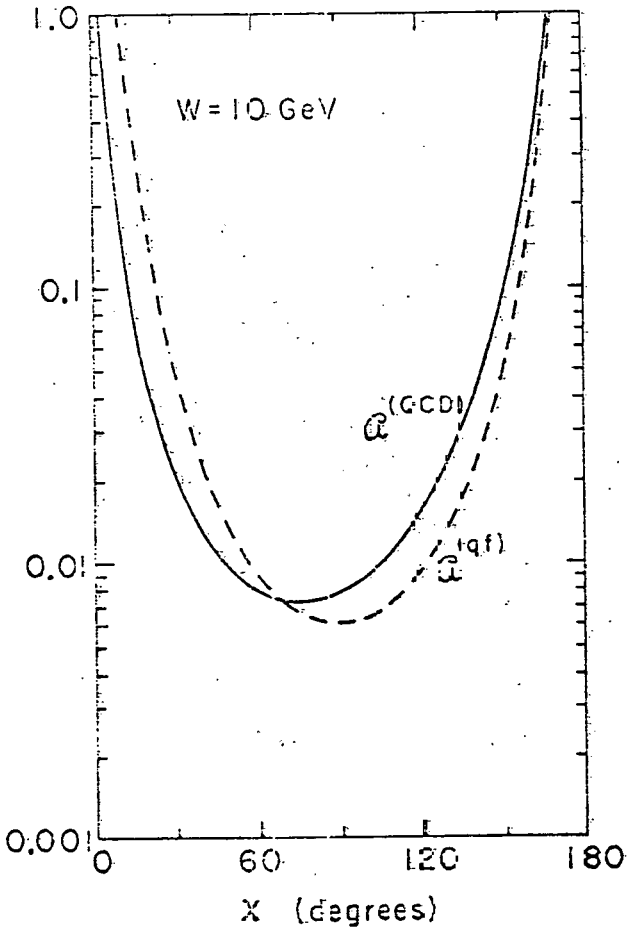
1.0
0.1
0.01
0.001
W = 10 GeV
$a^{(QCD)}$
$a^{(qf)}$
0
60
120
180
X (degrees)

Fig. 6 (a)

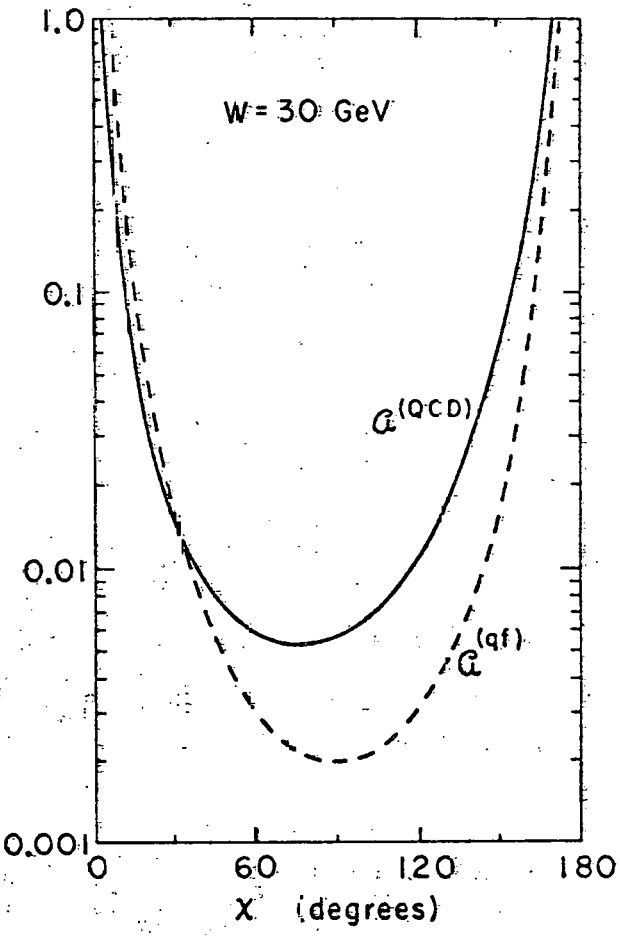
1.0
0.1
0.01
0.001
W = 30 GeV
$a^{(QCD)}$
$a^{(qf)}$
0
60
120
180
X (degrees)

Fig. 6 (b)

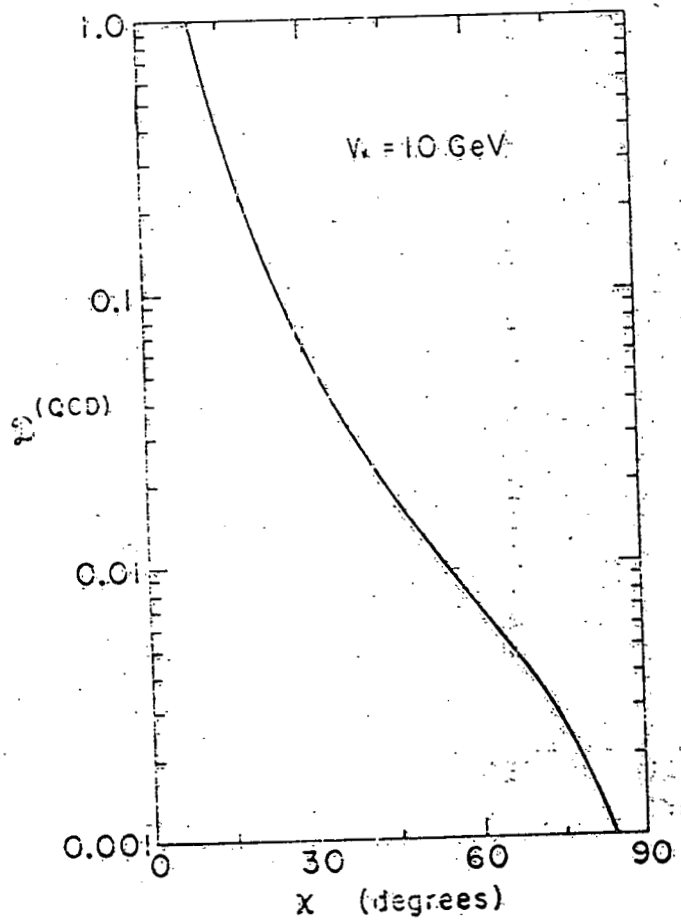
1.0
0.1
0.01
0.001
$\mathcal{B}^{(QCD)}$
$V_\perp$ = 10 GeV
0
30
60
90
χ (degrees)

Fig. 7

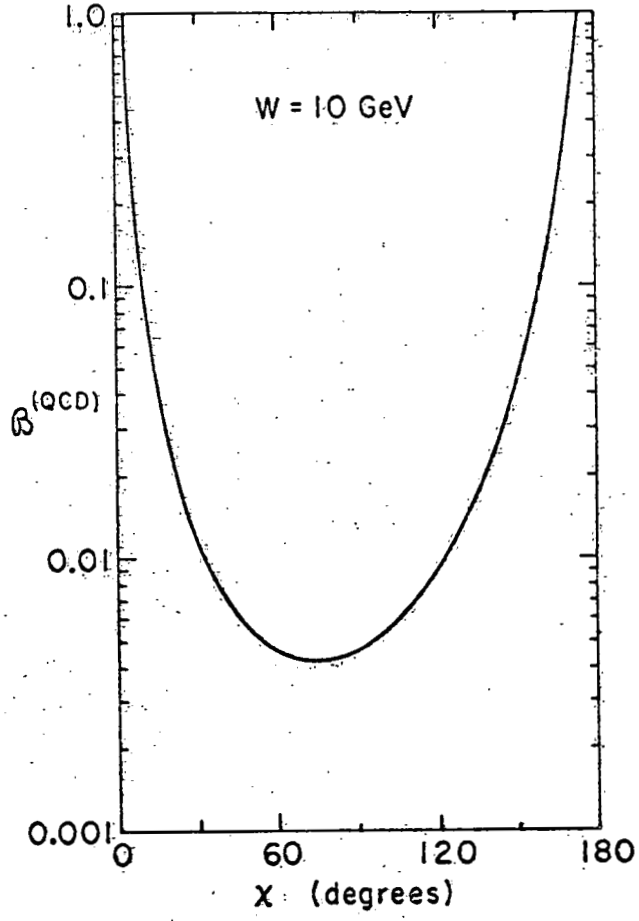
1.0
0.1
0.01
0.001
$\mathcal{B}^{(QCD)}$
W = 10 GeV
0
60
120
180
χ (degrees)

Fig. 8

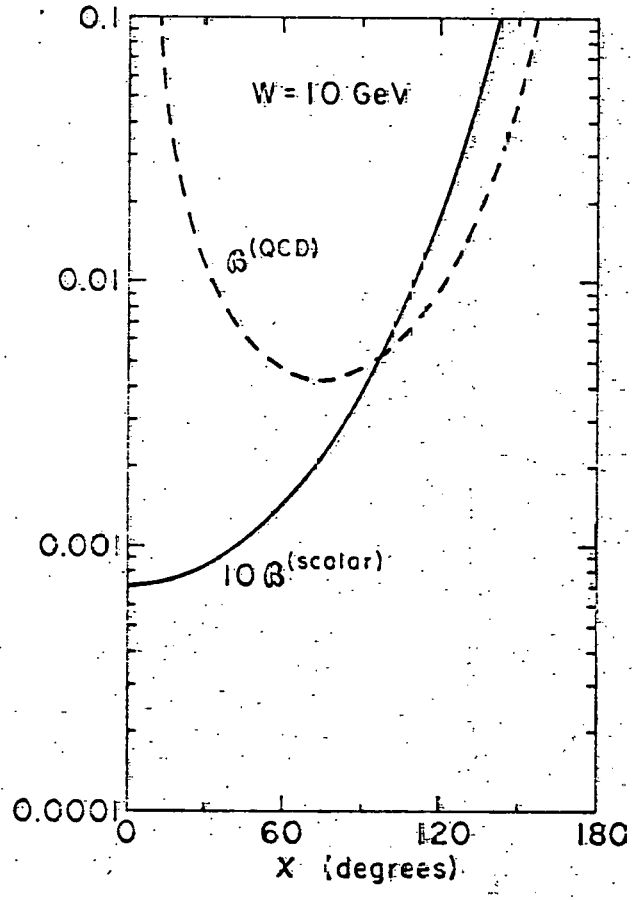
0.1
0.01
0.001
0.0001
W = 10 GeV
$\mathcal{G}^{(QCD)}$
$10\,\mathcal{G}^{(scalar)}$
0
60
120
180
X (degrees)

Fig. 9